DOI: ADD DOINUMBER HERE

An Innovative Strategy for Paraffin-based Fuels Reinforcement: Part II, Ballistic Characterization

Riccardo Bisin[⋆†]*, Christian Paravan*[⋆]*, Alberto Verga*[⋆] *and Luciano Galfetti*[⋆]
[⋆]*Politecnico di Milano, Aerospace Science and Technology Dept.,*
Space Propulsion Laboratory (SPLab)
34, via LaMasa, 20156, Milan, Italy
riccardo.bisin@polimi.it · christian.paravan@polimi.it · alberto.verga@.polimi.it · luciano.galfetti@polimi.it
[†]Corresponding author

Abstract

Low regression rate is nowadays the main issue of hybrid rocket engines (HREs). The exploitation of paraffin-based fuels could be the answer to this problem. In the present study, ballistic behavior of HTPB and paraffin-based fuel blends are studied and compared with the one of the *armored grains*, new generation of fuels featuring 3D-printed cellular structures embedded in the paraffin grain. Regression rate measurements are performed by means of thickness over time (TOT) approach. Armored grain combustion performance makes this novel fuel an interesting candidate for high-performance hybrid rockets.

1. Introduction

Hybrid rocket engines (HREs) are nowadays regarded as a promising propulsion solution for different aerospace applications spanning from in-space navigation to access to space and space tourism [1]. Even though the simplicity, intrinsic safety, reduced recurring costs, and, low environmental impact, the use of HREs is still hindered by the slow regression rates. This drawback is related to the diffusion nature of the flame in HREs implying low thrust level and hampering the hybrid rocket technology implementation in operating systems.
To cope with this problem, commonly employed solutions are the increment of the burning area by means of dedicated grain shapes, the enhancement of the turbulence in the combustion chamber, the exploitation of energetic additives, and the use of liquefying fuels, such as paraffin waxes [2].
Generally, multiport or non-conventional grain design can be difficult or expensive to be pursued. Recently, additive manufacturing has emerged as a method to rapidly and inexpensively produce almost any conceivable shape [3]. Turbulence generators and swirl oxidizer flows have been also studied to increment regression rate. Shin et al. [4] embedded metal wires in the grain promoting the turbulence. Vortex hybrid engine featuring swirl oxidizer flow was conceived by Knuth et al. [5] and a regression rate increment of 640% was achieved. Paraffin-based fuels represent a low-cost and effective solution for the enhancement of r_f thanks to the entrainment phenomenon [6]. During the combustion, these low-melting fuels are prone to create a thin liquid layer at the grain fuel surface. The oxidizer flow destabilizes the melted fuel layer due to the low viscosity and the low surface tension of the latter. As a result of the hydrodynamic stress, fuel droplets are entrained in the oxidizer core flow. The addition of this mechanical effect increases the r_f of liquefying fuels up to 3-4 times with respect to conventional polymeric fuels (e.g., HTPB) with vaporization as the only regression mechanism [7]. In their studies, Karabeyoglu et al. extended the classical Marxman's hybrid combustion theory to account for entrainment [8].
However, the paraffin waxes alone are not suitable for withstanding loads associated to hybrid rockets manufacturing, handling, and operation. For that reason, paraffin fuels mechanical properties should be enhanced. This goal is generally achieved by blending wax with polymers. On one hand, the structural performance can be improved, but on the other, the fuel melt viscosity and the surface tension are also increased hindering or suppressing the entrainment capability. As a consequence, the regression rate of high-viscous fuel formulations is lowered [9].

In this regard, several research groups are seeking the best compromise between fuel mechanical properties and regression rate enhancement. The Space Propulsion Laboratory (SPLab) of Politecnico di Milano is active in the re-

search on hybrid fuel ballistics. In particular, SPLab designed a lab-scale hybrid rocket engine with non-conventional configuration [10] and developed paraffin-based solid fuel formulations with reinforcing agents extensively tested at lab-scale [11]. The final goal is identifying the most suitable paraffin-polymer fuel grain fulfilling both mechanical and ballistic requirements. In this regard, a new approach of reinforcing paraffin fuels has been conceived exploiting the use of 3D-printed materials providing mechanical support for the paraffin and serving as an additional fuel component. In the present work, the ballistic behavior of the so-called *armored grain*, a paraffin grain reinforced with a 3D-printed gyroid structure, is discussed and compared with other paraffin-based fuels. The structural assessment of armored grain has been addressed in [12]. Please, refer to [12] for the gyorid production methodology and its selection as the most suitable reinforcement structure for paraffin fuels.

2. Investigated Fuels

In the study, different hybrid rocket fuels were tested. The ballistic investigation focused on three different groups of solid fuels: conventional polymeric fuel (HTPB), liquefying fuel formulations based on a commercial microcrystalline paraffin wax (SasolWax 0907), and the novel armored grain family. All the tested fuel formulations were loaded with 1 wt% carbon black (CB) and they are listed in Table 1.

Hydroxyl terminated polybutadiene (HTPB) is a thermosetting polymer widely used in the rocket industry. It can be considered the baseline for the comparison of the ballistic performance with other fuel formulations. The HTPB binder is based on HTPB-R45 supplied by Avio Spa. The binder is prepared adding a plasticizer (dioctyl adipate, DOA), a curing agent (isophorone diisocyanate, IPDI) and a curing catalyst (dibutyltin diacetate, TIN).

Both plain and blended paraffin-based fuels were investigated. The blend exploits styrene-ethylene-butylene-styrene grafted with maleic anhydride copolymer (SEBS-MA) as reinforcing agent to overcome the issue of wax poor mechanical properties. The formulation is 89% SasolWax 0907- 10% SEBS-MA- 1% CB (fuel id. S10W1). The composition is expressed in terms of percentage by weight.

The investigated armored grains feature a gyroid lattice structure embedded in the SasolWax 0907. The gyroids were printed by means of a commercial FDM 3D-printer following the *infill gyroid* methodology (refer to [12]). The ballistic test campaign focused on different polymers for the reinforcement structure. Polylactic acid (PLA), Acrylonitrile Butadiene Styrene (ABS), Nylon (NY) were selected as the material for the gyroid. The reinforcement structure is supposed to burn with the paraffin. The armored grains feature different materials for the gyroid but the same gyroid geometry for each grain. In particular, the gyroids have a 15% relative density $\tilde{\rho}$[1], that in turn corresponds to the volumetric fraction of polymer inside in the fuel grain. Since the 15% infill results the most promising from a mechanical viewpoint [12], the armored grain combustion tests were focused on this infill percentage for PLA, ABS and Nylon gyroids. The tested fuels are reported in Table 1. It should be noted that the compositions are expressed in terms of percentage by volume, which does not coincide exactly with the percentage by weight because of the different density of SasolWax 0907 and the gyroids material (PLA, ABS, NY). For further details about the solid fuel ingredients and the grain manufacturing, refer to [12].

3. Experimental Setup and Procedures

The combustion tests were performed with the SPLab lab-scale HRE. The facility is design to burn single-perforated cylindrical grains in a vertical configuration (see Fig. 1). The cylindrical specimen sizes are nominally 5 mm port diameter, 30 mm external diameter and 50 mm length. The facility features a water-cooled brass nozzle with throat diameter of 4 mm. The grain ignition is achieved by a pyrotechnic primer charge, while the pressure evolution in time is measured by a piezoresistive pressure transducer. The signal produced by the pressure transducer is recorded by an oscilloscope, which collects the pressure data (acquisition frequency 3 kHz) that are later analyzed during post-processing phase. The injector head is designed to swirl the flow and to accommodate a quartz window to allow the recording of the combustion with a high-speed camera at 500 fps. The sample head-end is visible during the test enabling the port diameter measurement from each of the recorded combustion images. Combustion tests are carried in gaseous oxygen GOX with an initial oxidizer mass flux G_{ox} of 250 kg/(m^{2}s). The oxidizer flow is regulated by a digital flowmeter. Gaseous N2 is used to quench the combustion before sample burnout. The oxygen and nitrogen lines are

[1] It is defined as the ratio between the density of the lattice ρ (i.e., the lattice mass divided by the occupied volume)

Table 1: Investigated formulations: HTPB, paraffin-based fuels and armored grains.

Fuel ID	Ingredients percentage, [%] SasolWax 0907	SEBS-MA	HTPB	PLA	ABS	Nylon	CB	Density (TMD)[a], ρ_f [kg/m^3]
HTPB[b]	-	-	99	-	-	-	1	921
W1[b]	99	-	-	-	-	-	1	929
S10W1[b]	89	10	-	-	-	-	1	928
W1_PLA_i15[c]	84	-	-	-	-	15	1	962
W1_ABS_i15[c]	84	-	-	-	-	15	1	947
W1_NY_i15[c]	84	-	-	-	-	15	1	944

[a]Density is reported as TMD (theoretical maximum density), not as actual density
[b]The ingredients fraction is considered as percentage by weight
[c]The ingredients fraction is considered as percentage by volume

commanded by two synchronized electrovalves enabling the simultaneous switch from oxygen to nitrogen.

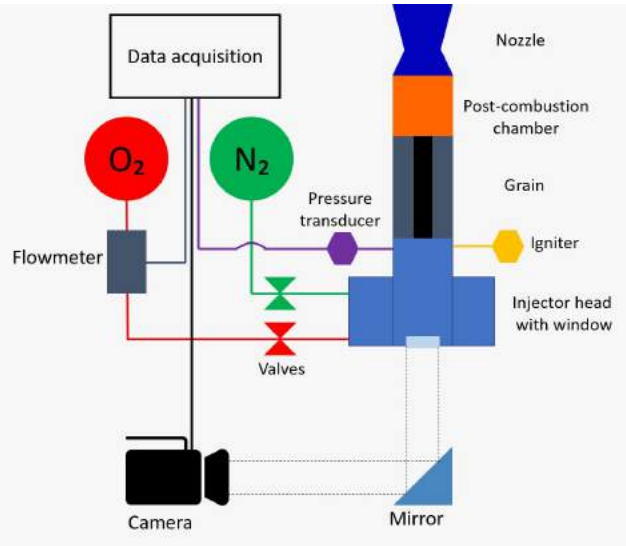

Figure 1: Schematics of the SPLab lab-scale hybrid rocket motor.

4. Regression Rate Measurement Techniques

Regression rate can be considered the most important figure of merit in HREs to assess the ballistic properties of the solid fuels. The solid fuel regression rate r_f is computed by mass-based and geometry-based thickness over time (TOT) approaches providing averaged ballistics. The analysis of the TOT approaches is based on the combustion time Δt_b. Pressure traces recorded during burning tests are analyzed to retrieve the combustion duration $\Delta t_b = t_{end} - t_{ign}$. Referring to Fig. 2, the ignition time t_{ign} is arbitrary chosen as the time at which the pressure reaches the 70% of the maximum value registered during combustion. This choice is done to avoid considering the contribution of the primer charge to the initial pressure rise into the combustion chamber after ignition. The end of the run is identified by the time t_{end} when nitrogen flow is purged into the combustion chamber.

In the present study, two TOT techniques were employed for the measurement of the regression rate r_f. The first is a mass-based (MB) TOT. The regression rate is computed as

$$r_{f,\mathrm{MB}} = \frac{\Delta m_b}{\rho_f \cdot A_{b,av} \cdot \Delta t_b} \tag{1}$$

Where Δm_b represents the difference in mass of the specimen before and after the combustion, while the average burning area $A_{b,av}$ is defined as

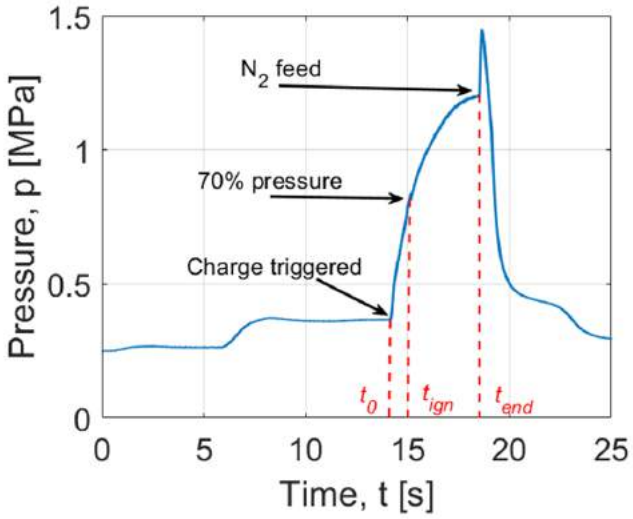

Figure 2: Typical pressure trace of a combustion run (W1_PLA_i15): t_0, t_{ign} and t_{end} are highlighted in red.

$$A_{b,av} = \pi \cdot \frac{D(t_0) + D(t_{end})}{2} \cdot L_{grain} \tag{2}$$

In Eq. (2), L_{grain} is the grain length before the firing and $D(t_0)$ and $D(t_{end})$ are respectively the port diameter before (t_0) and after (t_{end}) the combustion.

The geometry-based TOT approach is the second technique employed for the r_f measurement. It relies on the variation of the grain port diameter after combustion tests. The evaluation of the r_f by the diameter difference (DD) is computed as

$$r_{f,\mathrm{DD}} = \frac{1}{\Delta t_b} \cdot \frac{D(t_{end}) - D(t_0)}{2} \tag{3}$$

Finally, average oxidizer mass flux characterizing the firing tests is defined as

$$G_{ox,av} = \frac{G_{ox}(t_0) + G_{ox}(t_{end})}{2} = \frac{\dot{m}_{ox}}{2} \cdot \frac{4}{\pi(D^2(t_0) + D^2(t_{end}))} \tag{4}$$

5. Experimental Results and Discussion

The ballistic campaign was carried out considering:

- a conventional thermosetting fuel (HTPB);
- a pure microcrystalline wax fuel (W1);
- a reinforced formulation of the microcrystalline wax fuel exploiting 10% mass fraction of SEBS-MA (S10W1);
- three different types of armored grains featuring a 15% infill gyroid printed in PLA, ABS and Nylon (W1_PLA_i15, W1_ABS_i15, W1_NY_i15).

Three specimens were tested for each formulation. The ballistic results are reported in Table 2, while the regression rate variations with respect to HTPB are shown in Fig. 3. The relative grading of the ballistic performance for the solid fuels is enabled by the closeness of the experimental conditions. In particular, all the specimens feature comparable average oxidizer mass fluxes and average chamber pressure in the range 1.0-1.2 MPa.
The pure paraffin fuel (W1) exhibits a regression rate that is 2.5 times the one of the traditional HTPB. The addition of strengthening agents hinder the ballistic increment. A 10% SEBS-MA addition to the W1 reflects in a reduction of r_f, although this value is still slightly higher than the HTPB r_f. This evidence is in agreement with the statement that fuel formulations featuring the lower viscosity (W1) promote entrainment, and hence are characterized by the

fastest r_f. Regarding the armored grains, the r_f values are much higher than HTPB, and also greater than pure paraffin. Surprisingly, adding polymers in a gyroid-like shape to the fuel grain does not worsen the ballistic behavior of the paraffin fuel. On the contrary, the embedded gyroid structure enhances the r_f parameter. This underlines that the entrainment mechanism is not suppressed, even if a significant percentage of polymer is present inside the armored grains. Regression rate values for all the types of armored grains are comparable. However, the ABS-based armored grain (W1_ABS_i15) seems to be the most attractive from the ballistic viewpoint.
For all the formulations, both the MB and DD data enable the same relative grading. As far as r_f parameter is concerned, a difference between the mass-based (MB) and the diameter difference (DD) TOT approaches can be noted. This gap relies on the fact the latter method is based on the port diameter variation alone (see Eq. (3)) and it is not able to capture head-end burning observed in the fired grains (see Eq. 1). On the other hand, the head-end burning can be caught by the mass change method (MD) (see Fig. 4). For that reason, the $r_{f,\mathrm{MB}}$ values are generally higher than $r_{f,\mathrm{MB}}$ ones. This difference is more marked in paraffin-based fuels rather than in armored grains. Nevertheless, the comparison between $r_{f,\mathrm{MB}}$ and $r_{f,\mathrm{DD}}$ confirms how both the TOT techniques are suitable and effective for performing relative grading of the fuel ballistic characteristics.

Table 2: Results of the armored grains ballistic tests and comparison with HTPB, W1 and S10W1.

Fuel ID	$G_{ox,av}$, [kg/(m^{2}s)]	$r_{f,\mathrm{MB}}$, [mm/s]	$r_{f,\mathrm{DD}}$, [mm/s]	p_{av}, [MPa]
HTPB	129 ± 3	0.85 ± 0.07	0.69 ± 0.04	1.08 ± 0.16
W1	141 ± 4	2.08 ± 0.02	1.60 ± 0.01	1.23 ± 0.03
S10W1	130 ± 5	1.11 ± 0.07	0.89 ± 0.03	1.12 ± 0.02
W1_PLA_i15	128 ± 8	2.53 ± 0.01	2.16 ± 0.05	1.09 ± 0.02
W1_ABS_i15	132 ± 3	2.93 ± 0.12	2.76 ± 0.06	1.01 ± 0.05
W1_NY_i15	129 ± 3	2.77 ± 0.24	2.36 ± 0.24	1.08 ± 0.01

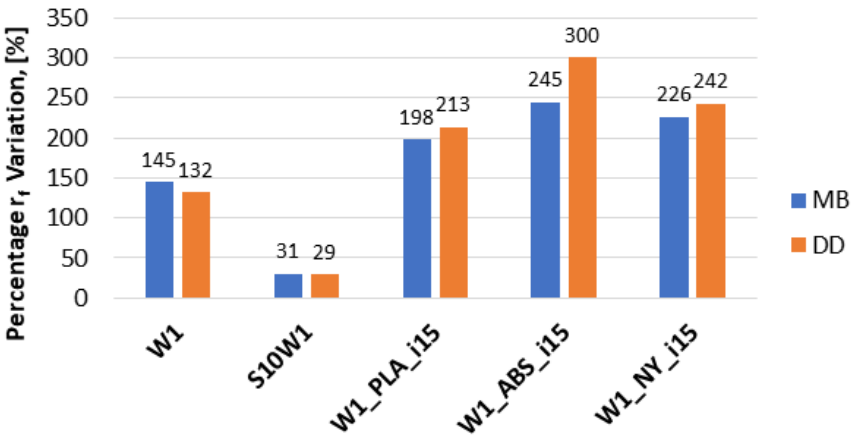

Figure 3: Percent regression rate variations of armored grains, W1 and S10W1 with respect to HTPB baseline. Regression rate is evaluated by means of MB (Eq. (1)) and DD approach (Eq. (3)). Test conditions: $G_{ox,av}$ = 135 ± 6 kg/(m^{2}s) and p_{av} = 1.1 ± 0.1 MPa

The r_f enhancement of armored grains might by caused by the turbulent flow promoted by the burnt embedded gyroid structure. Figure 5 shows the rough burning surface of the PLA armored grain. The roughness could increase the burning surface and promote turbulence, in turn increasing the regression rate and boost the mixing of reactants. The comparison between Fig. 4 and Fig. 5 evidences the different texture of the burning surfaces: smoothness for W1 and roughness for the armored grains.

As mentioned in Section 3, the lab-scale hybrid rocket engine is equipped with a quartz window to visualize the combustion and the fuel port area evolution. Some visualizations were recorder with a high-speed camera. In Figs. 6 - 9, different fuel formulations are reported. The images are equispaced in time and the first time instant t_{in} coincides with the fuel ignition, i.e., the moment in which the fuel port area becomes visible. The image sequences clearly show

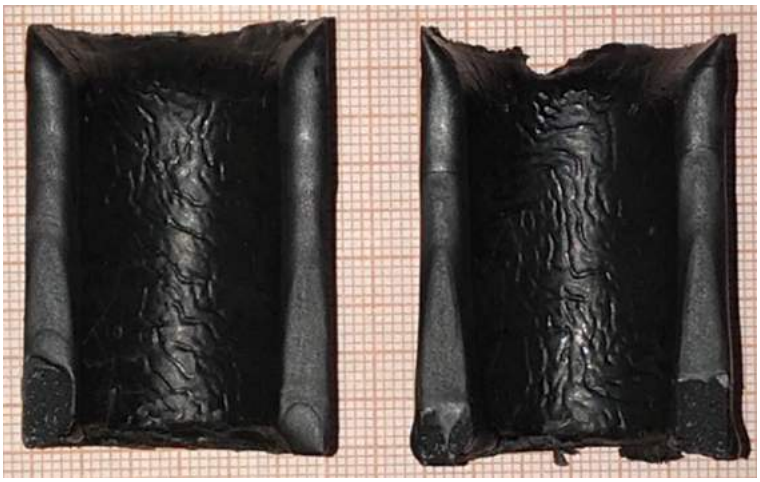

Figure 4: Cross-sectional view of a W1 fuel grain after firing. Oxidizer flows from top to bottom. Note the effects of the head-end burning on the strand inlet section.

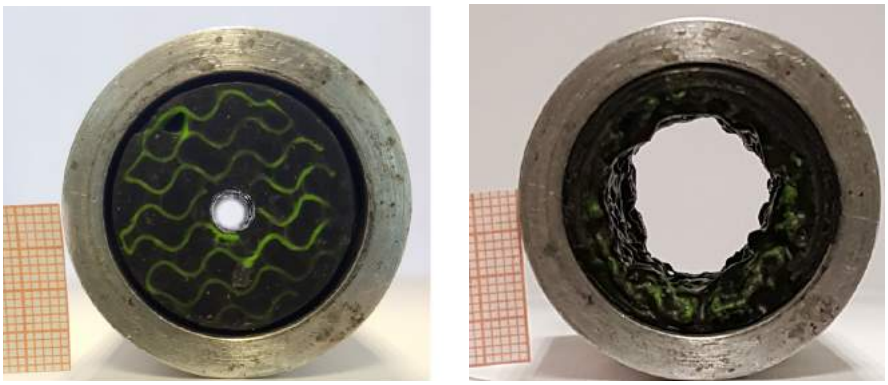

(a) (b)

Figure 5: PLA-armored grain W1_PLA_i15 before (a) and after firing (b). The oxidizer flow is direct outward.

that HTPB features the lowest r_f value, while W1 and W1_NY_i15 are the most attractive from the ballistic viewpoint. In fact, considering different formulations at the same time instant, W1_NY_i15 achieves slightly larger areas than W1. Port diameters difference between S10W1 and HTPB are negligible, suggesting similar ballistic performance. These results are in agreement with the ballistic data reported in Table 2.
It can be noted that W1, S10W1 and HTPB fuels are characterized by a circular port for all the combustion, whereas the armored grain features an irregular surface, in turn enhancing the turbulence inside the combustion chamber. This is also accentuated by the fact that the armored grain head-end is particularly involved in the combustion.

One critical aspect of paraffin-based fuels is represented by the slump under storage and operational conditions. This phenomenon could occasionally occur during combustion tests of paraffin-based fuels and SEBS-MA blends as reported in Fig. 10. This is mainly due to the presence of manufacturing flaws, caused by the paraffin shrinkage. Despite the possible presence of imperfections even in the armored grains, the paraffin slump was not observed during the armored grains combustion. In fact, although the regression surface is characterized by irregularities, the central port remains always quasi circular (Fig. 9). The gyroid reinforcement structures could prevent the detachment of large pieces (i.e., slump) of paraffin during the combustion.

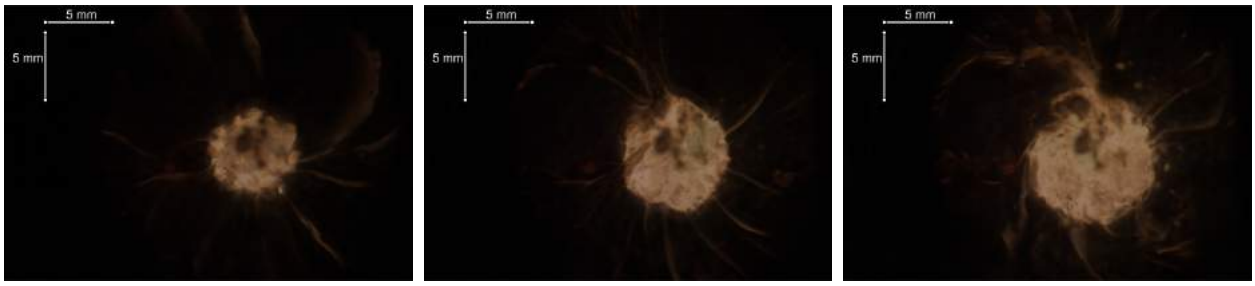

(a) $t = t_{in} + 0.70\ s$ (b) $t = t_{in} + 2.09\ s$ (c) $t = t_{in} + 3.49\ s$

Figure 6: Combustion of HTPB. The time instant t_{in} is the first moment in which the central port becomes visible.

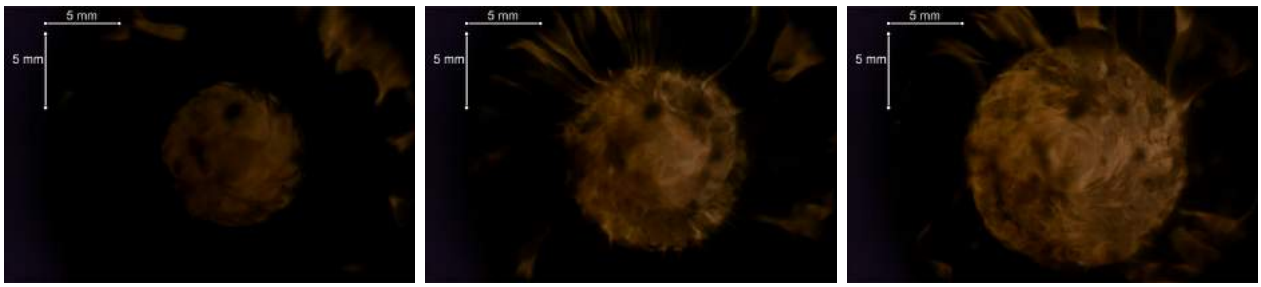

(a) $t = t_{in} + 0.70\ s$ (b) $t = t_{in} + 2.09\ s$ (c) $t = t_{in} + 3.49\ s$

Figure 7: Combustion of W1. The time instant t_{in} is the first moment in which the central port becomes visible.

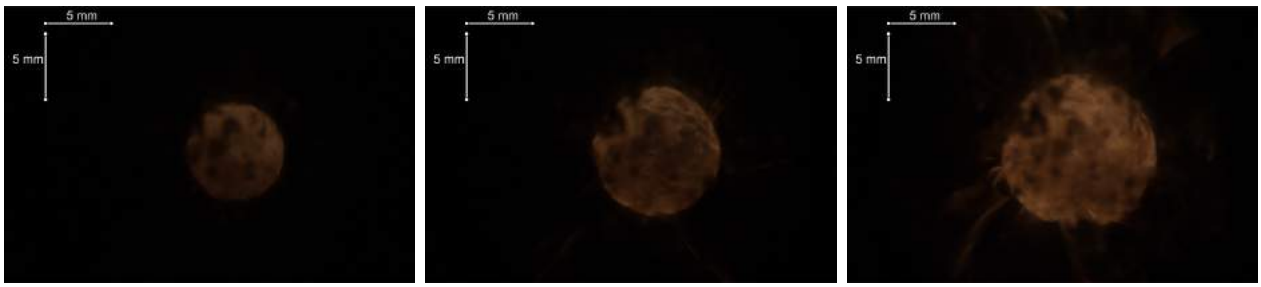

(a) $t = t_{in} + 0.70\ s$ (b) $t = t_{in} + 2.09\ s$ (c) $t = t_{in} + 3.49\ s$

Figure 8: Combustion of S10W1. The time instant t_{in} is the first moment in which the central port becomes visible.

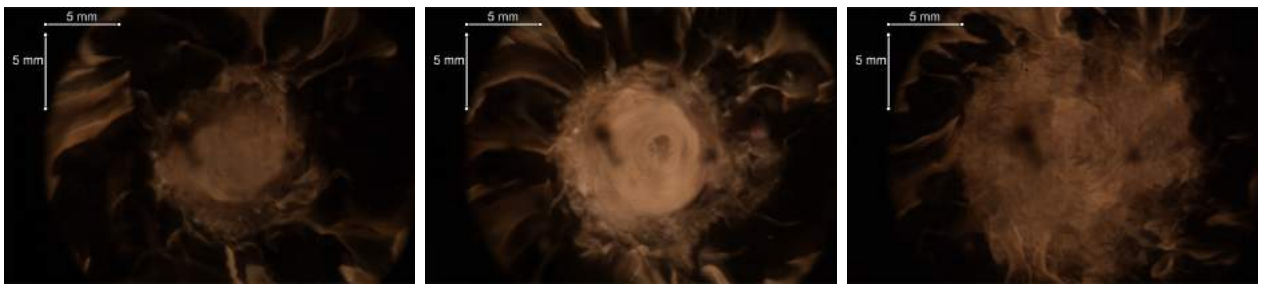

(a) $t = t_{in} + 0.70\ s$ (b) $t = t_{in} + 2.09\ s$ (c) $t = t_{in} + 3.49\ s$

Figure 9: Combustion of W1_NY_i15. The time instant t_{in} is the first moment in which the central port becomes visible.

6. Conclusions

The ballistic characterization of the armored grains, paraffin grains reinforced with a 3D-printed gyroid structure, was carried out in a lab-scale HRE with GOX as oxidizer. The investigated armored grains had approximately 15% lattice relative density and were made of PLA, ABS and Nylon. The ballistic results were expressed in term of regression

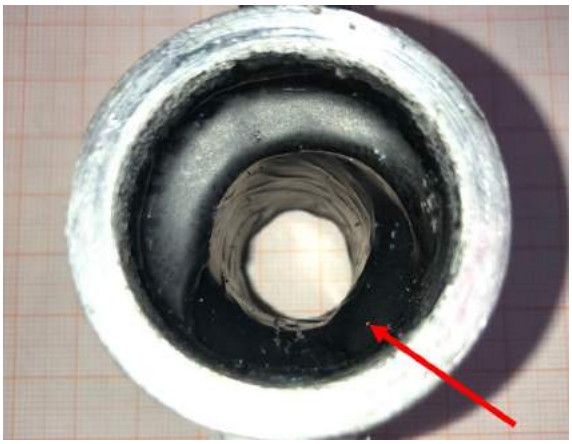

Figure 10: The slump of a paraffin-based fuel grain. The oxidizer flow is direct inward.

rate r_f values. Ballistic response of armored grains was compared with the one of HTPB and paraffin-based fuels. The firing tests revealed regression rates 22% to 41% higher than pure paraffin. Considering HTPB as a baseline, the regression rate increment ranged from 200% to 300%. Among the armored grains, the one that offered the best performance was the ABS-armored grain. The presence of the gyroid structure inside the paraffin fuel did not alter the paraffin melt layer viscosity hindering the entrainment. Moreover, during the burning, the surface of the grain featured an irregular contour, thanks to the presence of the gyroid. The roughness improved the convective heat transfer and hence the regression rate of the fuel.
The armored grain concept revealed to be the reinforcement strategy that not only saves the entrainment, but also provides augmented regression rate for paraffin-based fuels. The results make the armored grain a promising solution for the long-standing research for green paraffin-based fuels featuring both structural and combustion performance.

7. Acknowledgments

The Authors would like to acknowledge Marzia Zucchelli for the valuable support and assistance.

References

[1] D. Altman, "Overview and history of hybrid rocket propulsion," in *Fundamentals of Hybrid Rocket Combustion and Propulsion* (M. J. Chiaverini and K. K. Kuo, eds.), ch. 1, pp. 1–36, American Institute of Aeronautics and Astronautics, 2007.

[2] M. J. Chiaverini, "Review of solid-fuel regression rate behavior in classical and nonclassical hybrid rocket motors," in *Fundamentals of Hybrid Rocket Combustion and Propulsion* (M. J. Chiaverini and K. K. Kuo, eds.), ch. 2, pp. 37–126, American Institute of Aeronautics and Astronautics, 2007.

[3] M. A. Hitt, "Preliminary Additively Manufactured Axial-Injection, End-Burning Hybrid Rocket Motor Regression Rate Study," *2018 Joint Propulsion Conference*, pp. 1–5, 2018.

[4] K.-H. Shin, C. Lee, S. Y. Chang, and J. Y. Koo, "The Enhancement of Regression Rate of Hybrid Rocket Fuel by Helical Grain Configuration and Swirl Flow," *43rd AIAA/ASME/SAE/ASEE Joint Propulsion Conference & Exhibit*, no. AIAA-2005-0359, pp. 10–13, 2005.

[5] W. H. Knuth, M. J. Chiaverini, D. J. Gramer, and J. A. Sauer, "Solid-Fuel Regression Rate Behavior of Vortex Hybrid Rocket Engines," *Journal of Propulsion and Power*, vol. 18, no. 3, pp. 600–609, 2002.

[6] M. Karabeyoglu, D. Altman, and B. J. Cantwell, "Combustion of liquefying hybrid propellants: Part 1, general theory," *Journal of Propulsion and Power*, vol. 18, no. 3, pp. 610–620, 2002.

[7] M. A. Karabeyoglu, G. Zilliac, B. J. Cantwell, S. DeZilwa, and P. Castellucci, "Scale-up tests of high regression rate paraffin-based hybrid rocket fuels," *Journal of Propulsion and Power*, vol. 20, no. 6, pp. 1037–1045, 2004.

[8] M. Karabeyoglu and B. J. Cantwell, "Combustion of liquefying hybrid propellants: Part 2, stability of liquid films," *Journal of Propulsion and Power*, vol. 18, no. 3, pp. 621–630, 2002.

[9] C. Paravan, R. Bisin, S. Carlotti, F. Maggi, and L. Galfetti, "Diagnostics for Entrainment Characterization in Liquefying Fuel Formulations," *54st AIAA/SAE/ASEE Joint Propulsion Conference*, no. AIAA 2018-4830, pp. 1–12, 2018.

[10] C. Paravan, J. Glowacki, S. Carlotti, F. Maggi, and L. Galfetti, "Vortex combustion in a lab-scale hybrid rocket motor," no. AIAA 2016-4562, 2016.

[11] C. Paravan, L. Galfetti, and F. Maggi, "A Critical Analysis of Paraffin-based Fuel Formulations for Hybrid Rocket Propulsion," *53rd AIAA/SAE/ASEE Joint Propulsion Conference*, no. July, 2017.

[12] R. Bisin, C. Paravan, S. Alberti, and L. Galfetti, "An Innovative Strategy for Paraffin-based Fuels Reinforcement: Part I, Mechanical and Pre-Burning Characterization," *8th European Conference for Aerospace Sciences*, no. EUCASS 2019-718, 2019.